Chapter 12
Magnetic Core-Shell Nanoparticles for Biomedical Applications

Samir Mandal and Keya Chaudhuri

12.1 Introduction

Nanoscale objects are powerful devices in biotechnology medicine and biomedical sciences. They are potential applicants in recent clinical diagnostics and therapeutic techniques. Nanoparticles can be composed of numerous materials such as liposomes, polymeric micelles, block ionomer complexes, dendrimers, carbon, inorganic and polymeric nanoparticles, nanorods, quantum dots, iron oxide, gadolinium oxide, cadmium selenide–based quantum dots, and crystals of gold [1, 2]. Among these, iron oxide nanoparticles (IONPs) have drawn major attention, particularly for biomedical purposes thanks to their properties like biocompatibility, low toxicity, stability, availability for surface modification, and higher relaxation values. All have been tested preclinically or clinically for targeted drug and gene delivery and as agents to enhance diagnostic imaging output like in magnetic resonance imaging (MRI) [3]. Properties present only on the nanoscale level, like the increased intensity of fluorescent light emission of semiconductor crystals (quantum dots) or switchable magnetic properties of superparamagnetic iron oxide nanoparticles (SPIONs), make these materials unique and useful for applications in the biomedical field of medical imaging and cell tracking.

S. Mandal • K. Chaudhuri
Molecular Genetics Division, CSIR-Indian Institute of Chemical Biology, 4, Raja S. C. Mullick Road, Kolkata 700032, India
e-mail: kchaudhuri@iicb.res.in; keya.chaudhuri@gmail.com

S.K. Sharma (ed.), *Complex Magnetic Nanostructures*,
DOI 10.1007/978-3-319-52087-2_12

Without any surface modification, IONPs tend to agglomerate owing to their high surface-area-to-volume ratio, and aggregation results in the fast detection of nanoparticles by the immune system. To provide high colloidal stability and overcome the agglomeration tendency, coating is required on the surface of magnetic core-shell nanoparticles. Limitations associated with the utilization of IONPs in biomedicine are also overcome by coating the surface. For example, an appropriate coating substance can result in the dispersion of nanomaterials in biological surroundings, which may permit further functionalization of the surface, prevent nonspecific adsorption of plasma proteins on nanoparticles, improve compatibility in blood, and can hinder degradation by macrophages [4, 5].

Moreover, uncovered IONPs can be simply oxidized in air, resulting in the loss of magnetic and colloidal strength [6]. Surface coating of IONPs can be attained using various polymeric substances like polyethylene glycol (PEG), dextran, chitosan, polyvinyl alcohol (PVA), or starch [7, 8]. Furthermore, a few inorganic substances like gold or silica have also been used as a coating material [9]. Nowadays nonpolymeric organic substances like oleic acid, carboxylates, and alkyl phosphonates have also been used to coat the surface of IONPs [9].

IONPs smaller than 20 nm are bestowed with superparamagnetic properties and are therefore known as SPIONs. This supermagnetic property is vital for several applications in the biomedical field, and its uniqueness lies in the fact that as soon as the external magnetic field is removed, the magnetism of superparamagnetic materials is switched off. SPIONs are thus regarded as having high potential for a variety of uses in biomedicine, both for diagnosis and for therapy. For example, SPIONs can be used for MRI, early detection of inflammatory cancer and diabetes, hyperthermia, stem cell tracking, tissue repair, gene therapy, and manipulation of cell organelles [10]. Additionally, current studies have revealed the challenging role of surface-functionalized SPIONs in site-specific drug targeting [11]. The targeting potential of magnetic nanoparticles can be strengthened by immobilizing specific ligands on a surface, which is predicted to support the affinity of nanoparticles to the sites of attention. Such lignads are usually peptides, proteins, polysaccharides, antibodies, and aptamers [12]. Moreover, major progress in the internalization of nanoparticles by targeted cells can be achieved by choosing a proper ligand [13]. Intracellular delivery of curative drugs could be accomplished using stimulus-receptive coatings in the outer surface of nanoparticles. These advanced nanomachines are better in comparison to nontargeted ones and are expected to tackle current constraints on cancer treatment like nonspecific delivery of drugs in the body, unwanted health effects due to the necessity of a high dose to achieve the requisite high local drug concentration, cancer cells becoming resistant to drugs, and nonspecific toxic outcomes.

12.2 Types of Magnetic Core-Shell Nanoparticles

A magnetic core-shell nanoparticle, as the name implies, is a type of nanoparticle having a core or inner magnetic material and an outer shell composed of coating material. Varieties of core-shell nanoparticles have been prepared with diverse composition in close interaction and distinct use. The arrangement can be achieved by the interaction of inorganic/inorganic, inorganic/organic, and organic/inorganic materials. Normally, magnetic core-shell nanoparticles can be classified into two different categories as described below.

12.2.1 Magnetic Oxide Core Shell

Being of relatively inert surface composition, maghemite (or magnetite) magnetic nanomaterials generally do not allow for strong covalent bond formation with functional molecules. The use of silica as a shell on the surface of magnetic nanostructures has been reported to enhance the reactivity of magnetic nanomaterials. A variety of surface functional groups are employed to link with the silica shell through covalent bond formation. Functionalized silica-coated core-shell magnetic nanostructures can be utilized as fluorescence sensors through covalent bond formation with some fluorescent dye molecules [14].

Ferrite nanoparticle clusters, which are composed of approximately 80 maghemite superparamagnetic oxide nanocluster per bead with a silica shell, have a lot of advantages in comparison to metal nanoparticles. These are as follows: (1) superior chemical and thermodynamic stability, (2) precise size distribution, (3) higher colloidal stability, (4) dependence of the magnetic moment on the nanoparticle cluster size, (5) preservation of superparamagnetic properties regardless of cluster size of nanostructures, and (6) direct covalent attachment by the silica surface.

12.2.2 Metallic Magnet Core Shell

The material of a magnetic nanocore may be deactivated by gentle oxidation or the use of surfactants or polymers [15]. In an oxidative environment, an antiferromagnetic CoO layer was created on the surface of a Co nanoparticle. Recently, the exchange bias synthetic procedure was used to prepare a Co-core CoO-shell nanostructure coated with a thin gold outermost layer [16]. In addition, much attention has been paid to recently introduced nanoparticles having a magnetic core comprised either of metallic iron or cobalt with an inactive grapheme shell [17]. The benefits in contrast to ferrite or elemental nanoscale objects are (1) superior magnetization and (2) high stability in a wide range of pH and organic solvents.

12.3 Synthesis of Magnetic Core-Shell Nanoparticles

Magnetic core-shell nanoparticle synthesis is a two-step procedure. The first step is the synthesis of magnetic nanomaterials followed by encapsulation of the magnetic core materials with preferred organic or inorganic materials depending on the choice. The synthesis can be affected by a range of combinations such as organic/inorganic, inorganic/organic, and inorganic/inorganic materials in close affinity. The choice of shell materials in core-shell nanostructures is largely determined by the ultimate application and usefulness desired. Normally silica, various metals and nonmetallic oxides, drug molecules, and polymers are used as the coating substances.

The synthesis of magnetic IONPs with requisite characteristics is a challenging task for researchers, who must tackle two main challenges. First is the optimization of experimental conditions for generating monodispersed particles of the appropriate size, and second is reproducibility. Further purification procedures become necessary if the reaction product does not have a homogeneous and narrow size distribution. The aforementioned criteria are essential because the clinical potential of nanoparticles depends on monodispersity, shape, and size [7, 9]. Nowadays, numerous techniques have been adopted where efficient synthesis resulted in monodispersed, stable, and biocompatible nanoparticle populations. These techniques could be used to develop high-quality IONPs with the requisite size and shape. The most general methods for the synthesis of IONPs are coprecipitation techniques, microemulsion formation, hydrothermal synthesis, and thermal decomposition of iron complexes. Other methods, like electrochemical synthesis, sol-gel synthesis, laser pyrolysis, and sonochemical reactions, may be utilized for the synthesis of magnetic nanostructures [18]. In the present chapter, coprecipitation, microemulsion, hydrothermal synthesis, and thermal decomposition methods for the synthesis of IONPs are discussed in detail.

12.3.1 Coprecipitation Method

The slow addition of a base to a mixture of aqueous Fe^{2+}/Fe^{3+} salt solutions under an inert atmosphere at elevated temperature or room temperature could be employed for the synthesis of iron oxide (Fe_3O_4 or γ-Fe_2O_3) nanoparticles. This procedure is called the coprecipitation method since two ions are precipitated simultaneously. The magnetic property, composition, and morphology largely depend on the Fe^{2+}/Fe^{3+} ratio, concentration of sodium hydroxide, stabilizing agent, and temperature. If the synthetic reaction conditions are unaltered, the size, shape, and morphology of the magnetite nanoparticles are totally reproducible. However, in acidic pH, these nanoparticles are readily oxidized to a more stable maghemite form. The transformation of magnetite to maghemite is facilitated by forming acidic dispersion, followed by iron (III) nitrate administration. The maghemite particle is magnetically stable over a wide range of pH.

Though the magnetite particles are converted into maghemite form easily, the controlling narrow particle size distribution in Fe_3O_4, using the coprecipitation technique, is difficult. A broad range of particle size distribution with irregular magnetic activity would result if the blocking temperature fluctuates. The coprecipitation method is popular because of its simplicity and high yield in comparison to other methods of IONP preparation.

Magnetite (Fe_3O_4) or maghemite (Fe_2O_3) is produced in a reduction reaction of iron salts under alkaline conditions. For the synthesis of the magnetite form of iron oxide, aqueous solutions of ferric (Fe^{3+}) and ferrous (Fe^{2+}) ions are mixed in a 2:1 molar ratio and precipitated by the addition of a strong base like sodium hydroxide. The pH range of the solution must lie between 9 and 14 for efficient magnetite production. The magnetite particles are sedimented as a black solid. The stoichiometric chemical reaction for magnetite formation is given by

$$Fe^{2+} + 2Fe^{3+} + 8OH^{-} \rightarrow Fe_3O_4 + 4H_2O.$$

This reaction must be performed in an oxygen-free environment, since magnetite is very much prone to aerial oxidation [9]. Magnetite is transformed into more stable maghemite in the presence of oxygen directed as follows:

$$Fe_3O_4 + 2H^{+} \rightarrow \gamma\text{-}Fe_2O_3 + Fe^{2+} + H_2O.$$

In the presence of oxygen, magnetite (Fe_3O_4) particles can also be transformed into $Fe(OH)_3$ according to the following reaction:

$$Fe_3O_4 + 0.25O_2 + 4.5H_2O \rightarrow 3Fe(OH)_3.$$

The physical and chemical properties of nanostructures are affected by the oxidation/reduction priority of iron ions. Thus, an inert gas environment is required for carrying out the reaction. For example, an N_2/argon gas environment is required during the precipitation process, which can check the deterioration of Fe_3O_4. It is also observed that smaller particle sizes are associated with an oxygen-free environment during synthesis [6]. The size, shape, and morphology of nanoparticles can be regulated by modulating the type of salt (e.g., chlorides, sulfates, nitrates, perchlorates), the Fe^{2+}/Fe^{3+} molar ratio, the reaction temperature, the pH range of the solution, and the ionic strength of the medium [19]. The coprecipitation procedure is simple, fast, and of high yield and it produces nanoparticles with a wide range of sizes. To bypass the polydispersity of size, many efforts have been made. A coprecipitation synthesis method has been reported where the researchers were able to manipulate the size and homogeneity of the nanoparticles produced. Briefly, they controlled the pH of the ferrite solution uniformly using urea. The urea was decomposed by heating prior to the addition of the base to precipitate the iron

salts in the solution. A uniform particle size was associated with a consistent pH distribution of the ferrite solution. The mechanism of the reaction is as follows [20]:

$$CO(NH_2)_2 + H_2O \xrightarrow{\Delta} 2NH_3 + CO_2,$$

$$NH_3 + H_2O \rightarrow NH_4^+ + OH^-.$$

Since the decomposition of urea around 90 °C generates ammonia, and ammonia in water produces hydroxyl ions, increasing the pH of the solution. Thus alteration of the amount of urea might lead to the formation of a monodisperse nanoparticle population, resulting in a controlled IONP size.

12.3.2 Microemulsion Method

The coprecipitation method normally yields polydispersed particles; other techniques have been developed that give more control over nanoparticle dimensions. The microemulsion technique is one such alternative method producing IONPs with a narrow size distribution. The thermodynamically stable isotropic dispersion of two immiscible liquids in the presence of a suitable surfactant is a microemulsion technique. Water-in-oil reverse micelles have generally been employed for the synthesis of IONPs with narrow size distribution and uniform physical properties. Sodium bis(2-ethylhexylsulfosuccinate) (AOT), sodium dodecyl sulfate (SDS), and cetyltrimethyl-ammonium bromide (CTAB) and are the commonly used surfactants for the synthesis of IONPs [20]. Surfactant molecules generate a monolayer at the water and oil interface by the dissolution of hydrophobic parts of surfactant molecules in the oil phase and hydrophilic groups in the aqueous phase [6]. In this microemulsion technique, the aqueous solution is iron salts are dissolved in the core of the reverse micelle and the precipitation reaction is carried out inside the aqueous core. Thus, by manipulating the size of the aqueous core, one can adjust the nanoparticle size.

The synthesis of SPIONs with a narrow particle size distribution has been reported utilizing AOT/n-hexane reverse micelles in an N_2 atmosphere [21]. The size of the reverse micelle core was kept within the nanometer range, and as a result, SPIONs with a size of around 15 nm was obtained. In another study, using a microemulsion of cyclohexane/Brij-97/aqueous phase, the synthesis of SPIONs with a size distribution of 3.5 ± 0.6 nm with high magnetization values was achieved. The microemulsion technique produces a relatively good size distribution and shape control, and the use of potentially toxic surfactants makes this method bioincompatible. However, the aggregation and colloidal instability required further modification.

12.3.3 Hydrothermal Synthesis Method

A wide range of nanostructures can be synthesized by applying hydrothermal conditions. A liquid-solid-solution reaction has been employed for the synthesis of a diverse array of nanocrystals. The system employed for the synthesis consisted of a solid-liquid-solution matrix containing metal linoleate (solid), an ethanol linoleic acid (liquid), and a water-ethanol solution at different reaction temperatures under hydrothermal conditions [22]. This approach is based on phase transfer and a separation mechanism occurring at the liquid-solid-solution interfaces present during the synthesis. Using hydrothermal reduction, monodisperse, hydrophilic, single-crystal ferrite microspheres were synthesized. According to this process, a mixture of $FeCl_3$, sodium acetate, ethylene glycol, and PEG was stirred vigorously till a clear solution was formed, followed by sealing in a Teflon-coated stainless-steel autoclave, and heated to 200 °C for 8–72 h.

The aforementioned four synthetic methods have some advantages and disadvantages. Among the four methods, coprecipitation is the preferred route in terms of the simplicity of the synthesis. The thermal decomposition method can be considered the best in terms of controlling the size and morphology of nanoparticles. As a substitute, microemulsions can also be employed to synthesize monodispersed nanoparticles having various morphologies. However, a large amount of solvent is needed in this method. Hydrothermal synthesis, although it generates superior quality nanoparticles, is a comparatively little investigated method for the synthesis of magnetic nanoparticles. To date, magnetic nanoparticles are synthesized on a large scale by the use of coprecipitation and thermal decomposition procedures.

12.3.4 Thermal Decomposition

The synthesis of magnetic particles with the desired shape and size derived from the idea of quality semiconductor nanocrystals and oxide-nanoparticle synthesis involving a thermal decomposition technique using nonaqueous media [23]. Organometallic compounds upon thermal decomposition in high-boiling-point organic solvents with stabilizing surfactants produce monodisperse magnetic nanocrystals of smaller size [4]. In this process, the frequently used surfactants are fatty acids, oleic acid [24], and hexadecylamine [25]. Metal acetylacetonates [M(acac)n] (M = Fe, Mn, Co, Ni, Cr; n = 2 or 3, acac = acetylacetonate), metal cupferronates (MxCupx) [M = metal ion; Cup = N-nitrosophenylhydroxylamine, $C_6H_5N(NO)O$-], or carbonyls [26] can be used as organometallic precursors. The size and shape of a magnetic nanocomposite can be regulated by varying the ratio of the starting reagents including organometallic compounds, surfactant, and solvent. The reaction temperature, time, and aging period are also vital for the precise control of the size and shape of magnetic nanoparticles. If the metal is in a zero valent state, for example in carbonyls, thermal decomposition primarily tends to

lead to the creation of the metal; however, a two-step procedure is often used to make oxide nanoparticles. For example, at 100 °C, iron pentacarbonyl is capable of decomposing into a mixture of oleic acid and octyl ether, followed by the addition of a mild oxidant like trimethylamine oxide $(CH_3)_3NO$ at a higher temperature, and produces monodisperse γ-Fe_2O_3 nanocrystals approximately 12 nm in size [26]. Upon decomposition a precursor with cationic metal centers produces oxide nanoparticles. For example, Fe_3O_4 is formed upon decomposition of $Fe(acac)_3$ in the presence of oleoylamine, 1,2-hexadecanediol, and oleic acid in phenol ether [26]. The pyrolysis of metal fatty acid salts (such as salts of decanoic acid, lauric acid, myristic acid, palmitic acid, oleic acid, and stearic acid) in a nonaqueous solution (octadecene, n-eicosane, tetracosane, or a mixture of octadecene and tetracosane) generated size- and shape-controlled magnetic oxide nanocrystals [27]. This method provides nearly monodisperse Fe_3O_4 nanocrystals having a wide range of size-adjustable capacity (4–50 nm) with controlled shapes, including dots and cubes. This method has been successfully employed for the synthesis of Cr_2O_3, MnO, Co_3O_4, and NiO magnetic nanocrystals. Variation of the reactivity and concentration of the precursors is the key factor to control the size and shape of nanocrystals. Variation of the concentration and chain length of fatty acids determines the reactivity of the materials. Generally, a faster reaction rate is associated with a shorter chain length. Alcohols or primary amines are often employed to speed up the reaction rate and decrease the reaction temperature.

An analogous thermal decomposition procedure has been proposed for the production of monodisperse iron oxide nanostructures [28]. An iron oleate complex have been synthesized in situ using iron (III) chloride and sodium oleate and then thermally decomposed between 240 and 320 °C in various solvent systems such as 1-hexadecene, 1-octadecene, 1-eicosene, octyl ether, and trioctylamine. In this method, the particle size depends on the decomposition temperature and aging period. In this reaction, aging plays an important and necessary role in the production of IONPs. Nanoparticles synthesized by this method are capable of dispersion in various organic solvents, together with hexane and toluene. Monodisperse iron nanoparticles (6–15 nm) can be synthesized by decomposing iron pentacarbonyl and the iron oleate complex at different temperatures, and these can again be oxidized to magnetite [29]. This procedure is equivalent to seed-mediated growth and therefore can be explained by the classical LaMer mechanism.

In biotechnology applications, water-soluble magnetic nanoparticles are more advantageous. This requirement led to the preparation of water-soluble Fe_3O_4 nanocrystals with $FeCl_3 \cdot 6H_2O$ as an iron source and 2-pyrrolidone as a coordinating solvent under refluxing conditions (245 °C) [30]. In this method, the mean particle size is controlled at 4, 12, and 60 nm, respectively, when the reflux times are 1, 10, and 24 h. With increasing reflux time, a change in the shapes of particles from spherical to cubic morphologies was observed. Recently, water-soluble magnetite nanoparticles were synthesized using one-pot synthesis under analogous reaction

states with the addition of a surface capping agent like α,ω-dicarboxyl-terminated poly (ethylene glycol) [31]. These nanoparticles are used as MRI contrast agents for the diagnosis of cancer.

Metallic nanoparticles can also be prepared by a thermal decomposition method. Metallic nanoparticles have many advantages over other metal oxide nanoparticles owing to their larger magnetization. Thermal breakdown of $[Fe(CO)_5]$ in the presence of polyisobutene in decalin in a nitrogen atmosphere at 170 °C produces metallic iron nanoparticles [32]. Depending on the $[Fe(CO)_5]$/polyisobutene ratio, the size of the particle can be adjusted from 3 to 10 nm, with a polydispersity of approximately 10%. Susceptibility measurements revealed that the iron nanoparticles prepared in this way can be easily oxidized by exposure to air. This oxidation can generate a marginal increase in particle sizes approximately by a factor of 1.3. Iron nanocubes can be synthesized by the breakdown of $Fe[N(Si(CH_3)_3)_2]_2$ with H_2 in the presence of hexadecylammonium chloride or hexadecylamine and oleic acid at 150 °C [33]. The edge-length of the nanocubes varied from 7 to 8.3 nm along with the varying relative concentrations of amine and acid ligand. These nanocubes can accumulate into expanded crystalline superlattices by having their crystallographic axes aligned.

Cobalt nanoparticles can also be prepared by the thermal decomposition method. Their shape and morphology both can be controlled by this method [34]. Cobalt nanodisks can also be prepared by the thermal decomposition of a cobalt carbonyl precursor [35]. The high-temperature reduction of noncarbonyl organometallic complexes produces cobalt nanorods [36] and nickel nanorods [37]. For example, the decomposition of $[Co(H_3\text{-}C_8H_{13})(H_4\text{-}C_8H_{12})]$ with H_2 in anisole at 150 °C in the presence of a combination of hexadecylamine and a fatty acid (lauric, octanoic, or stearic acid) produces monodisperse ferromagnetic cobalt nanorods. The variation of diameter and length of the cobalt nanorods largly depends upon the different acids used [36].

Magnetic alloy nanoparticles have many advantages over other magnetic nanoparticles owing to their enhanced magnetic susceptibility, high magnetic anisotropy, and large coercivities. Besides $CoPt_3$ and FePt, metal phosphides have generated a lot of interest in nanotechnology and chemistry [38]. Hexagonal iron phosphide and related materials have been thoroughly studied for their ferromagnetism, magnetoresistance, and magnetocaloric effects [39]. Recently, iron (III) acetylacetonate and manganese carbonyl with tris(trimethylsilyl) phosphane at elevated temperatures have been exploited to prepare FeP and MnP nanoparticles, respectively [40]. Further, the thermal decomposition of a precursor/surfactant mixture solution was applied to prepare antiferromagnetic FeP nanorods [41]. Using a syringe pump technique and thermal decomposition of iron pentacarbonyl in trioctylphosphane generates distinct iron phosphide (Fe_2P) nanorods.

12.4 Functionalization of Magnetic Nanoparticles by Natural/Synthetic Polymers

For the synthesis, storage, and use of IONPs, their stability is extremely important. Bare nanoparticles generally agglomerate and form clusters, reducing their large surface area. Surface coating imparts colloidal stability and prevents agglomeration. To achieve further functionalization and targeting, the selection of appropriate coating material is essential and nanoparticles can be designed as soluble in biological media. The desirable properties of coating materials include the high chemical affinity of iron oxide core, nonimmunogenicity, nonantigenicity, and protection from opsonization by plasma proteins [42].

According to literature reports, many different polymeric coating materials have been found to be used, among those the present review focuses on coatings with PEG, PVA, chitosan, and dextran, as these polymeric materials have been most commonly used [43].

12.4.1 Polyethylene Glycol

PEG is a synthetic polymer, which is often preferred in nanoparticle functionalization because of its several advantages, especially for biomedical uses. First, it is a biocompatible polymer having a hydrophilic nature and therefore can be dissolved in water. The US Food and Drug Administration (FDA) has approved the biocompatibility of PEG [44]. Second, there are reports that PEG enhances the biocompatibility of iron oxide nanostructures and removes fast blood clearance, increasing the blood circulation time of nanoparticles, ultimately benefitting drug release applications. PEG coating further enhances the internalization competence of nanoparticles into cells [45]. Apart from its excellent solubility and stability in aqueous media, it is also stable in physiological saline [9]. The only disadvantage of a PEG coating is its nonbiodegradability in the human body; the metabolic clearance of PEG is so far not fully known [46].

PEG coating has usually been achieved either during or after the preparation of nanostructures. Nanostructures coated with PEG following a synthesis reaction have been shown to possess better dispersion profiles than those coated with PEG during synthesis reactions [47]. A number of methods are available in the literature for coating IONPs with PEG. A chemical coprecipitation method has been described as a facile route to synthesize PEG-coated Fe_3O_4 nanoparticles [48]. This procedure involves the mixing of PEG with ferric and ferrous sulfate as precursor, which was subsequently precipitated simultaneously by the addition of base. Another two-step approach has been described that is comprised of IONP synthesis by a coprecipitation method, followed by coating with PEG by the addition of PEG solution to an iron oxide suspension and stirring for 24 h [49]. PEG hydrogel–coated IONPs have been prepared by surface-initiated photopolymerization reactions [50].

In this process, a prepolymer solution composed of PEG, accelerator, initiator, and water and then exposed to green light using an argon ion laser to initiate the photopolymerization reaction.

12.4.2 Polyvinyl Alcohol

PVA is another popular coating material used usually for biomedical applications, for several reasons. First, it is biocompatible and hydrophilic in nature. Second, it has low toxicity and resists the aggregation of nanoparticles in a biological environment [45]. In addition, synthesis procedures in the presence of PVA lead to the formation of monodispersed particles. The multihydroxyl structure of PVA results in its enhanced crystallinity, culminating in necessary thermomechanical properties like high elastic modulus, crystallinity, and tensile strength in bioapplications [45]. PVA has the interesting property of retaining its elastic modulus even with high water content in hydrogels. Therefore, it is appropriate for a number of applications ranging from drug delivery to wound healing [51]. It has been shown that PVA-coated IONPs have drawbacks in tissue penetration [52].

12.4.3 Chitosan

Chitosan is a cationic polysaccharide having structural similarities with cellulose. It is made up of 2-amino-2-deoxy-H-D-glucan linked with glycosidic linkages. Owing to the presence of primary amine groups, chitosan has a great importance in pharmaceutical applications. Its mucoadhesive property and positive charge have made it attractive for drug delivery applications. Chitosan is not water-soluble in basic or neutral pH conditions, whereas in acidic pH with amino groups being protonated, chitosan becomes water-soluble. Chitosan does not elicit an allergic reaction and is regarded as biocompatible. It is capable of biodegradation, leading to the formation of nontoxic amino sugars [9]. It has found applications in affinity protein purification and magnetic bioseparation. Owing to these features, chitosan-coated IONPs are regarded as promising candidates for tissue engineering applications [53].

There are a number of studies on chitosan-coated IONPs for biomedical applications. Chitosan-coated nanoparticles synthesized by a controlled coprecipitation method yielding particles 12 nm in size showed superparamagnetic properties and were therefore suitable for biomedical applications. Another study reported the synthesis of IONPs coated with chitosan followed by modification of the surface of the particles with PVA [54]. This hybrid coating system had low protein adsorption because of its surface zeta potential and is regarded as a promising candidate for in vivo drug delivery applications.

12.4.4 Dextran

Dextran is an essential material that has been used for coating IONPs for fundamental applications like MRI, cancer imaging, and cancer treatments [42]. Dextran coating on SPIONs has been clinically approved in the MRI of liver [55]. Dextran, although biocompatible in nature, is not degradable in the human body since dextranase, the enzyme degrading dextran, cannot be synthesized by human cell lines [56]. One of the disadvantages of dextran coating is the formation of weak bonds with IONP surfaces, which affects applications negatively [42]. Another disadvantage of dextran is its unfavorable effect on compound tolerance, which leads to limited infusion in a slow process [57].

Various reports about the dextran coating of IONPs for biomedical applications are available in the literature. Dextran-coated monocrystalline IONPs have been used for the intracellular magnetic labeling of various target cells [58]. IONPs were treated with epichlorohydrin to crosslink dextran preventing dissociation under certain biological conditions. Further functionalization of the surface was also carried out by ammonia. The derivatized particles were found to be internalized into cells over 100-fold more efficiently than nonmodified particles [58]. In another study, the synthesis of dextran-coated IONPs conjugated with bombesin was produced as a targeting contrast agent for breast cancer imaging using MRI. A one-step coprecipitation method was used for the synthesis of 6 nm dextran-coated IONPs where dextran was mixed with iron salts, which were precipitated with ammonia. The system was shown to possess good diagnostic advantage in mice with breast tumors [59].

12.5 Biomedical Applications

Over the past 20 years, IONPs have been used for various biomedical applications, including MRI, tissue repair, detoxification of biological fluids, immunoassays, hyperthermia, drug delivery, gene delivery, cell tracking, bioseparation, cell separation, and manipulation of cellular organelles. In recent years, new techniques have been used to functionally acclimatize nanoparticles for clinical applications. In this chapter, these approaches, their current limitations, and developments have been explained in detail.

12.5.1 Imaging Applications of IONPs

12.5.1.1 Photoacoustic Imaging

In the past few decades, fluorescence and bioluminescence imaging have been used mostly in vivo to envisage biological tissues. The limitation of these systems

is due to their attaining simultaneously high spatial resolution and adequate penetration depth [60]. Photoacoustic imaging (PAI), also called optoacoustic or thermoacoustic imaging, is a potential new area with the prospect of overcoming this limitation.

The photoacoustic effect, which is the basis of PAI, was first reported by Alexander Graham Bell in 1880 by the recognition of sound produced by light [61]. The photoacoustic effect in this context refers to the production of ultrasound (acoustic) waves following the adsorption of electromagnetic radiation by tissue chromophores, and these ultrasound waves in turn generate images of tissues based on the extent of the optical absorption [60]. In this way a depth of a few centimeters with a scalable spatial resolution is possible, which offers elevated contrast and greater spatial resolution at the same time. However, the photoacoustic effect has developed widely in the last decade for biomedical applications like breast, skin, and cardiovascular system imaging [61].

In an ideal PAI, the optical absorption of the preferred object needs to be enhanced for better image contrast, while for deeper signal dissemination, the optical absorption of normal tissues must be low [62]. Many studies have focused on finding contrast agents, and currently contrast agents are considered to be of two types: endogenous and exogenous. The most popular endogenous agents are melanin and hemoglobin [63, 64]. Indocyanine green (ICG), gold nanoparticles, single wall nanotubes (SWNTs), quantum dots (QDs) and fluorescent proteins were reported as the most widespread exogenous contrast agents [62, 65].

The benefits of using endogenous agents for imaging are their safety and ability to demonstrate proper physiological conditions. Endogenous agents cannot be used for visualization of nonvascularized tissues, although they are capable of visualizing vasculature tissues [60]. Furthermore, they are insufficient for the recognition of early-stage tumors [62]. As a result, exogenous contrast agents like gold nanoparticles are essential for improved PAI. Note that most frequently used exogenous agents have limitations in accomplishing efficient and precise targeting [60].

For this purpose, gold-coated IONPs are useful for preparing dual mode nanoparticle having ability for photoacoustic imaging with MRI simultaneously [66]. The shell thickness and surface properties of IONPs must be regulated accurately since they establish magnetic attraction, photon scattering, near-infrared (NIR) absorption, and added biomolecular conjugation [67].

Many studies have proposed the direct coating of gold onto IONPs [68]. For example, hybrid nanoparticles with an iron oxide core and a gold nanoshell have been synthesized and characterized [69]. These nanoparticles showed superparamagnetic properties and a significant absorbance in the NIR region, which is essential for successful PAI. It has been demonstrated that gold coating on IONPs normally produces particles larger than 100–200 nm in diameter with uneven surfaces, which negatively influences the MRI response [67]. These observations led to the recent report of a synthesis of SPIONPs coated with a gold shell by generating a gap between the core and the shell [67]. The results illustrated that these nanoparticles are bestowed with extremely integrated characteristics, including

electronic, magnetic, optical, acoustic, and thermal properties. This strategy created a contrast agent with excellent MRI and PAI capabilities, and the procedure is known as magnetomotive photoacoustic (mmPA) imaging.

12.5.1.2 Magnetic Resonance Imaging

The past decade has seen increased applications of MRI. However, MRI agents need to enhance image contrast among normal and diseased tissue in order to distinguish healthy tissues from pathological ones. A variety of contrast agents have been proposed. So far, paramagnetic contrast drugs, such as paramagnetic gadolinium chelates, have been exploited in MRI experiments [70]. These drugs are known to function by shortening the T1 relaxation time (longitudinal relaxation time) of water in tissues. Alternatively, superparamagnetic nanoparticles enhance diagnostic specificity and sensitivity owing to their finer properties, for instance higher molar relaxivities and ability to reduce both T1 relaxation time and T2 transversal relaxation time [71]. The competence of these particles is determined by their size, charge, and coating material, and they can be improved by the additional alteration of their surface properties using certain biologically active materials such as specific antibodies, receptor ligands, polysaccharides, and proteins [72, 73].

A few SPIONs, such as Feridex, Resovist, Sinerem, and Clariscan, were accepted for clinical applications some time ago [74]. Feridex with dextran coating (hydrodynamic size 120 nm) has been reported to be used for cellular labeling and liver imaging. Resovist, coated with carboxydextran (hydrodynamic size 60 nm), has been utilized for liver imaging. Sinerem has found several applications, such as in the imaging of metastatic lymph nodes, areas of macrophages, and as blood pool material. The size of Sinerem lies between 15 and 30 nm together with its dextran coating. Clariscan has also been used in blood pooling and has a coating of around 20 nm of PEGylated starch [9]. However, these commercial contrast agents cannot be altered further for tissue targeting purposes. At present, several studies have focused on generating novel MRI contrast materials, where a number of approaches have been used to attain the requisite targeting capability [75, 76]. For example, a superparamagnetic MRI contrast agent coated with dextran has been used to target endothelial inflammatory adhesion molecule E-selectin [77]. The use of a synthetic mimetic of sialyl Lewisx, a natural ligand of E-selectin expressed in leukocytes, further functionalized the contrast agent in vitro (on cultured human umbilical vein endothelial cells) and in vivo (on a mouse model of hepatitis).

A new MRI contrast drug for in vivo cancer imaging was reported recently. The contrast agent was designed to contain an antibiofouling polymer that is thermally cross-linked with SPIONs (Fig. 12.1) but holds no targeting ligands on its surface. This agent has been found to accumulate in tumor cells [78]. Surface coating layers on the nanoparticle enhance permeability and retention, providing significant tumor detection. This new contrast material has been demonstrated to deliver anticancer drugs to tumors with high competence. Therefore, it has proven useful as a drug delivery carrier, which may be advantageous equally for cancer imaging and therapy.

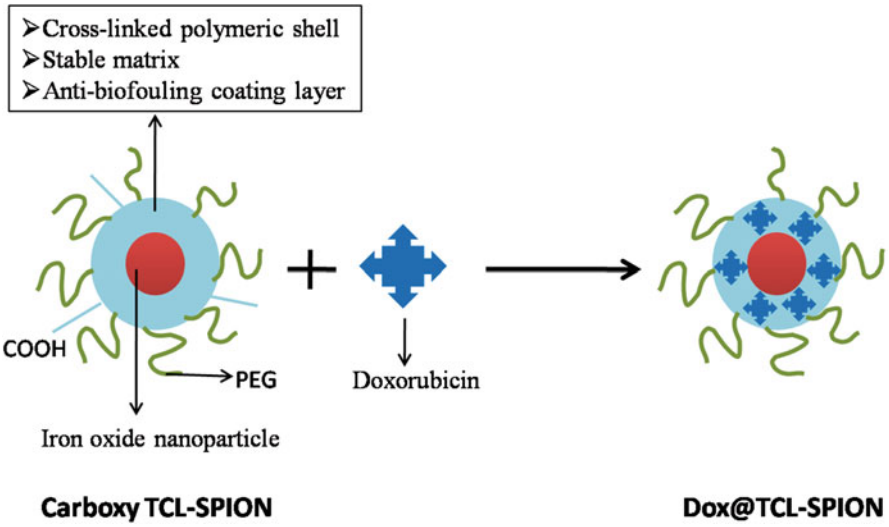

Fig. 12.1 Schematic diagram showing drug-conjugated antibiofouling polymer coated with thermally cross-linked SPIONs

In vivo experiments on animal models established that elevated amounts of SPIONs accumulated in the tumor microenvironment, and drug release kinetics in vitro proved that within 50 min 60% of the drug was released.

The synthesis of multifunctional SPIONs was reported and found use in targeted drug delivery and positron emission tomography (PET)/MRI [79]. Doxorubicin (DOX), cRGD, PET 64Cu chelators, and tumor targeting ligands were linked onto PEGylated SPIONs. The efficacy of this structure as a contrast agent for MRI was examined in an in vitro study using MRI relaxivity. Interestingly, these new contrast agents could assemble in the tumor region in greater amounts compared with free cRGD, the MRI relaxivity being comparable to that of Feridex. These multifunctional SPIONs can be exploited for both cancer therapy and PET/MRI [79]. Moreover, in vivo experiments demonstrated that 64Cu-labeled cRGD-conjugated SPIO nanocarriers gathered in the tumor region but not in normal tissues.

12.5.2 Drug Delivery

The limitations in drug delivery involve the absorption of hydrophobic drugs as well as site-specific targeting of the drug. Targeted delivery depends on the improved efficacy and biocompatibility of the drug. As a result, the design of appropriate delivery vehicles for drug release at specific sites and significant absorption of the drug by specific cells will be crucial advancements in therapeutics. Nanoparticle-based drug delivery is emerging as a growing field due to its remarkable features,

like small size, along with the strong physical properties of the nanomaterials [72, 80]. The superparamagnetic behavior of nanoparticles depends on their size. Another vital aspect of SPIONs is the lack of permanent magnetization, which helps nanoparticles to preserve their colloidal stability [81]. Since a critical level of magnetization is necessary for biomedical applications, there needs to be a tradeoff between the minimum size to prevent aggregation but still have enough magnetization to retain the magnetic application [81]. Nanoparticles, because of their small size, can easily penetrate into peripheral tissue with effective enhanced permeation and retention (EPR), especially in the case of cancer [81]. The penetration power of nanoparticles through leaky vasculatures can be used for the design of drug targeting vehicles. Nanoparticles can be encapsulated with therapeutic molecules through surface attachment or entrapment [82]. Other advantages include the reduction of multidrug resistance (MDR), which occurs especially for hydrophobic drugs. MDR is caused by an ATP binding cassette (ABC), which is a transporter generally overexpressed in cancer cells, that pumps hydrophobic drugs out. SPIONs can be used in conjunction with DOX to overcome MDR as well as to increase the efficacy of drug delivery [83].

For the delivery of magnetic nanoparticles, one must use either magnetic force or passive targeting strategy. Passive targeting is effected using the reticuloendothelial system (RES), a very important clearance system in the body. As bare nanoparticles enter the body, they are exposed to opsonins, which are plasma proteins identifying nonself structures, and nanoparticles, because of their high surface tension, readily attach to opsonins. The extent of attachment depends on the nanoparticle size, shape, and aggregation state and the surface charge. For example, nanoparticles greater than 250 nm are cleared readily by RES clearance and move from the bloodstream into the spleen [81]. Further, nanomaterials 10–100 nm in size are cleared by liver cells, while nanoparticles of less than 10 nm are cleared renally [84]. The optimal size range of nanoparticles for drug delivery applications has been suggested to be 10–100 nm because the bloodstream clearance time for this size range is higher compared to other sizes of nanomaterials [81].

Active targeting means the functionalization of nanoparticles by different targeting agents [85]. The procedure consists of the adhesion of coating/targeting molecules to the structure followed by the loading of drugs. There are different ways of loading, for example, covalent conjugation or physical adsorption [81]. In one of the early clinical trial and release studies, human serum albumin microspheres coated with magnetite-containing doxorubicin were used as anticancer agent [86]. Later, these trials continued with epidoxorubicin-conjugated magnetic nanoparticles [87].

For improved colloidal stability, various nanoparticle stabilizers with adequate biocompatibility have been used. Organosilane molecules with amine groups such as (3-aminopropyltriethoxysilane) APTES and APTMS are some examples [82]. Other compounds, like silica derivatives, which are chemically inert, have not been used in biological applications.

There are various studies on drug conjugation on SPIONs, especially IONPs, involved in both imaging and drug delivery. SPIONs functionalized with reversibly bound drugs have the potential to be delivered to specific sites [46]. The synthesis of IONPs having a dimension of 10 nm and with enormous colloidal stability is by functional polymers capable of attaching DOX through a pH-sensitive imine bond formation [88]. This bond cleaves in acidic pH, making the nanomachine suitable for potential targeting in a tumor environment, which is acidic in nature. Two- and three-dimensional cell models of IONP uptake and intracellular release of DOX demonstrate that this MRI negative contrast drug is suitable for both diagnosis and therapy. The delivery of antibiotics like ofloxacin and ciprofloxacin from APTES-coated IONPs has been demonstrated [82]. Further, starch derivative–covered IONPs functionalized with phosphate groups have been used in chemotherapy that targeted mitoxantrone to the tumor site [89]. In addition, other nanocomposite designs are found in the literature, where SPIONs and quantum dots find application in the targeted delivery of camptomicin, an anticancer agent [90].

In recent times, an insulin-loaded iron oxide–chitosan nanohybrid has been synthesized and the prospective drug delivery potential of the nanomaterial was examined through an oral delivery route for the management of type II diabetes [91]. Interestingly, the insulin-loaded iron oxide–chitosan nanocomposite could lower blood glucose levels by more than 51% in mild diabetic, subdiabetic, and severely diabetic rats. Another report showed promising results for hybrid magnetic nanogels composed of SPIONs modified by chitosan and CdTe quantum dots [92]. Spherical hybrid nanogels smaller than 160 nm were utilized for insulin delivery and found to be promising for insulin delivery as well as for cell imaging purposes.

The molecular markers overexpressed in cancer cells can be utilized for specific targeting strategies. For example, in breast cancer cells, HER2 receptors are overexpressed, and conjugation of anti-HER2 antibody onto nanoparticle surfaces was used for selective targeting [93]. Similarly, folic acid has been used for targeting HeLa and MCF7 cells [94]. Tumor endothelial cells are known to express cell surface receptors for angiogenesis [46]. One such target, avb3 integrin, plays a key role in endothelial cell survival during angiogenesis. Ligands like Arg-Gly-Asp (RGD) peptide for targeting avb3 integrin on cell surface have been utilized for SPION attachment [46]. CREKA also targets fibrin and is found mostly around tumor areas in the case of selected tumor types [95].

12.5.3 Cell Tracking

Specific cell tracking could be another possible application of IONPs. To label and track cells under in vivo conditions, adequate quantities of magnetic nanoparticles must be introduced into the cultured cells. Under these conditions, cell tracking can be obtained at a resolution close to the size of the cell. This requires the conjugation of cell-permeable peptides or transfection agents onto the negatively charged surface of the nanoparticles [9]. To enhance SPION uptake by cells, nanoparticles can be

additionally functionalized with some specific peptides, or peptides coated with dendrimers, which increase cellular internalization [96, 97]. Stem cell tracking and tracking of immune cells and (T) lymphocytes have been demonstrated by this technology [98].

IONPs having a diameter of around 50 nm have been synthesized with silica coating. For proper labeling and tracking of human mesenchymal stem cells (hMSCs), fluorescein isothiocyanate (FITC)-conjugated IONPs were prepared. The labeling was performed by clathrin- and actin-dependent endocytosis followed by intracellular localization in late endosomes/lysosomes [99]. These bifunctionalized nanoparticles can generate adequate MRI contrast, while the viability and proliferation of the labeled stem cells are unaltered. Another report suggests labeling and tracking mesenchymal stem cells (MSCs) and hematopoietic (CD34+) stem cells through ferumoxide–protamine sulfate complexes. The authors demonstrated that labeled cells showed no short- or long-term toxicity and showed comparable cell proliferation with unlabeled cells [100].

MRI cell tracking of rat T-cells under in vivo conditions was carried out by labeling them with superparamagnetic dextran-coated iron oxide particles [101]. Tissue inflammation was induced, which attracted labeled T-cells by adding calcium ionophore. This study provided the first of its kind of a successful cell tracking in vivo by MRI. The experiments of immune cell tracking is comprised of additional targeted strategies with additional functionalization through transfection agents. In this way, T-cells were tracked in vivo by introducing SPIONs derivatized with a peptide sequence from transactivator protein (Tat) of HIV-1 into cells [102]. MRI, fluorescence-activated cell sorting, and biodistribution analysis demonstrated that T-cells were proficiently labeled and tracked with these superparamagnetic agents with no alteration of their normal activation.

12.5.4 Magnetic Fluid Hyperthermia

Magnetic fluid hyperthermia (MFH), where an alternating magnetic field is used to release a drug to the proper site, has often been used for cancer therapy. This alternating field generates heat, which effectively releases the drug inside tissue or cells and sometimes the heat affects the cellular mechanism, resulting in the destruction of the solid tumor. A hyperthermia agent serves as energy absorber to convert into cytotoxic heat energy and specifically destroy tumor cells since tumor cells are more vulnerable to heat compared to healthy cells [103]. Hence, for the treatment of tumor cells, magnetic nanoparticles have great importance. The magnetic induction of magnetic nanoparticles can be done by irradiation with microwaves, sound waves, and radio frequency waves [104]. The magnetic moments of superparamagnetic nanoparticles are free to fluctuate in response to thermal energy owing to their single-domain low energy state, and this makes them suitable for hyperthermia applications. Their small size and unique magnetic properties make SPIONs promising candidates. The Curie temperature, the temperature at

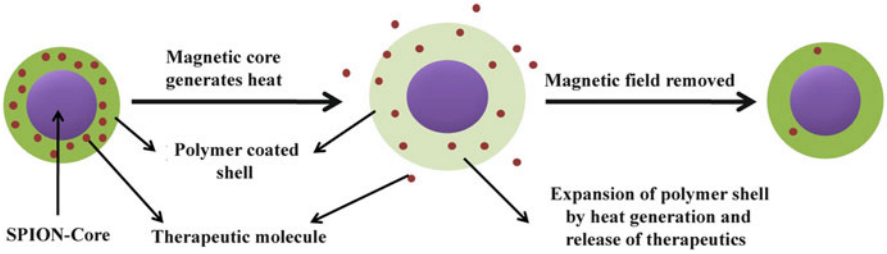

Fig. 12.2 Schematic diagram of drug release mechanism during hyperthermia treatment

which magnetic materials lose their permanent magnetic properties and convert to diamagnetic materials, is almost 100 °C for SPIONs [89]. However, SPIONs are essentially coated with PEG/PVA/chitosan/dextran/aminosilane to cope with biocompatibility issues [45, 105].

The first hyperthermia experiment exploiting paramagnetic materials dates back to 1957. In that early experiment, a 1.2 MHz magnetic field was utilized for IONPs to achieve a size of up to 100 nm [106]. A regional hyperthermia application was run clinically on prostate cancer and considered to be a first trial [107]. Later on, microparticles of iron oxide doped with yttrium were used for MRI combined with hyperthermia to treat liver cancer [108].

Hyperthermia management combined with drug release was performed using folic acid and beta cyclodextrin–functionalized IONPs [109]. The drug was fit into the system (Fig. 12.2) using beta cyclodextrin through hydrophobic interactions. The release of the drug was affected by applying high-frequency magnetic fields that heated the system up to 42–45 °C. This helped to depress the hydrophobic interaction between the drug and beta cyclodextrin, thereby releasing the drug. Therefore, in this temperature range, both drug and hyperthermia treatments occur concurrently [109].

Further, hyperthermia has some restrictions. First, hyperthermia is more successful as a local application instead of a regional one. Second, the application is only promising at a fixed temperature range of 42–45 °C for local hyperthermia [110]. Also, the released heat should be such as to target a specific site rather than healthy cells. Thus, optimizations of the size and colloidal stability of nanoparticles are critical for clinical application of magnetic fluid hyperthermia therapy [110, 111].

12.5.5 Gene Delivery

Gene delivery can be done using viral or nonviral vectors. Viral vectors, owing to their toxicity and severe immune response, are not favored in general. Nonviral gene delivery strategies, like needle and jet inoculation, hydrodynamic gene transfer, gene gun, electroporation, and sonoporation, are not competent enough for transfer of

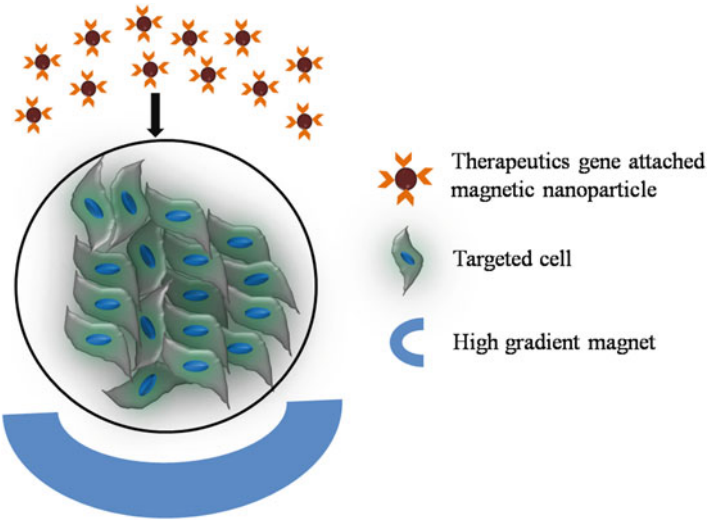

Fig. 12.3 Schematic representation of external magnetic field–directed gene delivery in vitro using magnetic nanoparticles

genes [112]. Gene therapy has been applied primarily for genetic disorder–related diseases, especially for immune system–linked diseases, for example, chronic granulomatus disorder and severe combined immune deficiency, for neurodegenerative disorders like Parkinson's disease and Huntington disease, and in a range of cancers [113]. The aim of gene delivery is to replace or silence the defective gene causing the disease. The constraints are on the delivery of genes to the specific target, and there is difficulty in examining the subsequent target response [114].

Recently, magnetic nanoparticles have emerged as a promising candidate for gene delivery, both in vitro and in vivo. The strategy, known as magnetofection, has been employed by linking therapeutic genes onto magnetic nanoparticles, which are then targeted to specific sites through high gradient external magnetic fields (Fig. 12.3) [115]. This specific system has two benefits in vivo, first by facilitating external magnetic field–induced sedimentation, and second, by external magnetic field–directed targeting of tumor sites for gene delivery. Magnetic nanoparticles release genes either by enzymatic degradation or by hydrolysis of the polymer coating around the nanocore [115]. IONPs are capable of gene transfection at targeted sites by external magnetic induction [116]. For the binding of negatively charged plasmids, positively charged coating materials, such as PVA, polyethylenimine (PEI), and chitosan, have been used [117]. For example, for targeted delivery of DNA from magnetic nanoparticles, adeno-associated virus (AVV), encoding green fluorescent protein (GFP), and a cleavable heparin sulfate linker have been used [118].

12.5.6 Bioseparation

Magnetic separation is widely utilized in biotechnology, and in recent times it has been the most useful application of magnetic nanoparticles. Quite a few magnetic nanoparticle types have been synthesized for this purpose, but novel and advanced techniques, which can be used in the case of dilute solutions of targeted molecules, must be explored [119]. SPIONs have been used in a magnetic separation technique for the separation of proteins and cells. Traditional separation techniques, for example, various chromatography techniques and ultrafiltration, are more complex and costly in comparison to magnetic separation processes. Additionally, a purification process in the magnetic separation technique with SPIONs can be achieved with only one test tube, resulting in great simplicity in comparison to other procedures [9].

In the magnetic separation procedure, affinity ligands to attract specific targets are immobilized on the surface of nanoparticles. Then, the addition of target molecules to the sample will lead to purification or separation. Following an incubation period, magnetic nanoparticles attach to the specific target molecule and subsequently be simply extracted from the sample with an external magnetic field (Fig. 12.4) [119]. The beauty of this technique lies in its direct application to crude materials and its efficient separation of small particles. For protein isolation,

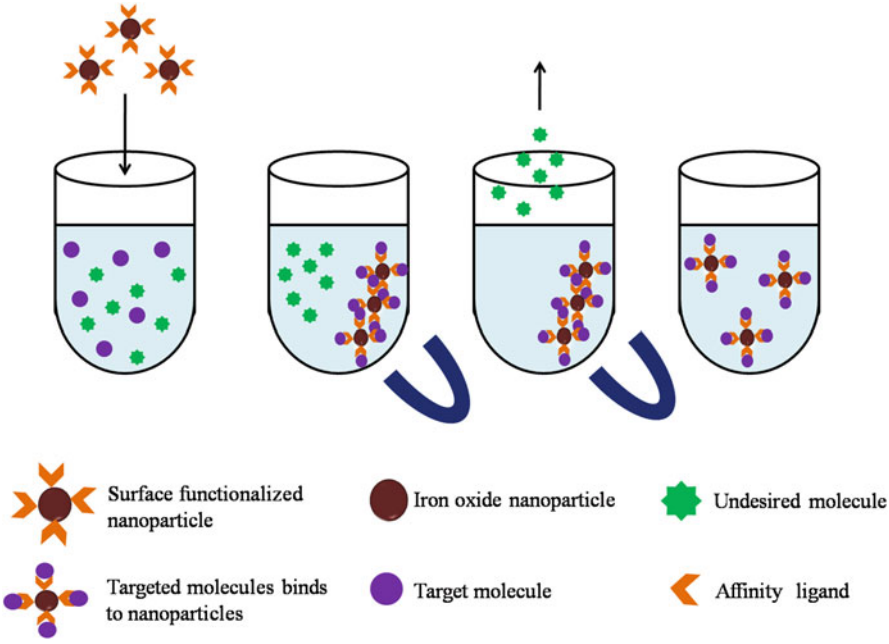

Fig. 12.4 Schematic representation showing external magnetic field directed separation

the affinity ligands are streptavidin, nitrilotriacetic acid, antibodies, proteins A and G, trypsin, and trypsin inhibitor [120]. A small permanent magnet can be enough, though stronger rare-earth magnets are also commercially available [119].

For the isolation of avidin protein, superparamagnetic γ-Fe_2O_3 nanoparticles have been synthesized via a site-exchange reaction [121]. Oleic acid–protected nanoparticles were further functionalized with charged bipyridinium carboxylic acids and biotin. Bipyridinium significantly improved the water solubility of nanoparticles, while biotin, which has high affinity for avidin, was utilized for surface localization. A new method for the transformation of cells followed by the selection of transformed cells using a magnetite cationic liposome (MCL)/DNA complex has been reported. Here, MCLs were associated with a plasmid vector, and the transformants were detached with an external magnetic field [122].

12.5.7 Tissue Repair

Wound healing in the body involves the joining of tissues at the damaged site, and the generation of tissue rejoining is facilitated by temperatures greater than 55 °C [123]. Laser systems are currently being used to induce heat inside tissues, which, however, leads to tissue necrosis in the applied region [124]. To minimize tissue damage, less harmful wavelengths and low-power lasers must be employed [56]. In this connection emerged the use of IONPs for tissue repair, and this procedure is known as soldering or welding. In this technology, two tissue surfaces are brought near, and then the merging of the tissues is increased by placing IONPs in between, and finally the requisite amount of heat is supplied to the tissue-nanoparticle system. It is desirable to use gold or silica coatings because there is strong absorbance of light. In this way, wavelengths causing minimum harm to tissues and higher-wavelength lasers have been used.

12.5.8 Manipulation of Cellular Organelles

The magnetic manipulation of cellular organelles finds application in management from a distance without making contact. Nanoparticles are functionalized with particular targeting agents for precise recognition by an organelle. It is essentially an attractive approach because it provides information on cell function and inherent signaling pathways. The manipulation of cytoskeleton, lysosomes, and mitochondria through IONPs has been discussed in this chapter because these organelles were commonly considered for targeting purposes in previous studies.

The first example of organelle manipulation via IONPs is cytoskeleton manipulation. The structure of a cell is maintained by microtubules, the primary component of cytoskeleton, which is again regulated by a signaling pathway called Ran/RCC1. This was shown by conjugating IONPs with a regulatory protein,

RanGTP. Experiments were done with *Xenopus laevis* egg extracts, and it was shown that in the presence of a magnetic field, the direction of the microtubule fibers was determined by the direction of the external magnetic lines of force.

Lysosome is another organelle that can be manipulated by IONPs. When lysosome membrane permeability exceeds a critical value, cell death occurs. This phenomenon can be effectively utilized for killing cancer cells. IONPs 14 nm in size have been synthesized and coated with proteins recognizing the epidermal growth factor receptor (EGFR) [125]. EGFR is overexpressed in cancer cells, making it a suitable target. IONPs coated with target proteins were fast internalized in the lysosomes of cancer cells. When an alternating magnetic field is applied externally, IONPs cause heating of the lysosomes, eventually damaging the lysosomal membranes, which increased permeability and, finally, bring about cell death [125].

Another important organelle manipulated by IONPs is mitochondria. Mitochondria play significant roles in signaling, cellular differentiation, cell death, and growth. Therefore, the manipulation of mitochondria may lead to treatment for many diseases, including cancer. IONPs 50 nm in diameter coated with cytochrome c-specific binding aptamers have been synthesized for this purpose [126]. When these particles were inoculated in HeLa cells, they were all found to be targeted specifically to mitochondria and internalized rapidly. In the presence of an external static magnetic field, the viability of cancer cells diminished significantly [126].

12.6 Conclusion

In this chapter, we have summed up the functions of IONPs in biomedical applications. The exploitation of IONPs in PAI, MRI, drug delivery, cell tracking, magnetic fluid hyperthermia, gene delivery, bioseparation, tissue repair, and the manipulation of cellular organelles has been discussed in depth. Although remarkable progress has been made with the exploitation of IONPs, wide-ranging investigations are needed for long-term toxicity studies and clinical trials. The destinies of IONPs following in vivo treatment, like the exclusion route and retention time in specific organs, are a field of interest.

References

1. Mandal S, Hossain M, Devi PS, Kumar GS, Chaudhuri K (2013) Interaction of carbon nanoparticles to serum albumin: elucidation of the extent of perturbation of serum albumin conformations and thermodynamical parameters. J Hazard Mater 15:238–245
2. Mandal S, Hossain M, Muruganandan T, Kumar GS, Chaudhuri K (2013) Gold nanoparticles alter Taq DNA polymerase activity during polymerase chain reaction. RSC Adv 3:20793–20799

3. Bridot J-L, Faure A-C, Laurent S, Riviere C, Billotey C, Hiba B et al (2007) Hybrid gadolinium oxide nanoparticles: multimodal contrast agents for in vivo imaging. J Am Chem Soc 129(16):5076–5084
4. Sun S, Zeng H, Robinson DB, Raoux S, Rice PM, Wang SX et al (2004) Monodisperse MFe_2O_4 (M=Fe, Co, Mn) nanoparticles. J Am Chem Soc 126(1):273–279
5. Mandal S, Chaudhuri K (2012) A Simple method for the synthesis of ultrafine carbon nanoparticles and its interaction with bovine serum albumin. Adv Sci Lett 5(1):139–143
6. Gupta AK, Curtis ASG (2004) Lactoferrin and ceruloplasmin derivatized superparamagnetic iron oxide nanoparticles for targeting cell surface receptors. Biomaterials 25(15):3029–3040
7. Mahmoudi M, Simchi A, Imani M (2010) Recent advances in surface engineering of superparamagnetic iron oxide nanoparticles for biomedical applications. J Iran Chem Soc 7(2):S1–S27
8. Lin C-W, Tseng SJ, Kempson IM, Yang S-C, Hong T-M, Yang P-C (2013) Extracellular delivery of modified oligonucleotide and superparamagnetic iron oxide nanoparticles from a degradable hydrogel triggered by tumor acidosis. Biomaterials 34(17):4387–4393
9. Laurent S, Forge D, Port M, Roch A, Robic C, Vander Elst L et al (2008) Magnetic iron oxide nanoparticles: synthesis, stabilization, vectorization, physicochemical characterizations, and biological applications. Chem Rev 108(6):2064–2110
10. Sonvico F, Mornet SP, Vasseur SB, Dubernet C, Jaillard D, Degrouard J et al (2005) Folate-conjugated iron oxide nanoparticles for solid tumor targeting as potential specific magnetic hyperthermia mediators: synthesis, physicochemical characterization, and in vitro experiments. Bioconjug Chem 16(5):1181–1188
11. Nasongkla N, Shuai X, Ai H, Weinberg BD, Pink J, Boothman DA et al (2004) cRGD-functionalized polymer micelles for targeted doxorubicin delivery. Angew Chem Int Ed Engl 43(46):6483–6487
12. Dias A, Hussain A, Marcos AS, Roque ACA (2011) A biotechnological perspective on the application of iron oxide magnetic colloids modified with polysaccharides. Biotechnol Adv 29(1):142–155
13. Basuki JS, Esser L, Duong HTT, Zhang Q, Wilson P, Whittaker MR et al (2014) Magnetic nanoparticles with diblock glycopolymer shells give lectin concentration-dependent MRI signals and selective cell uptake. Chem Sci 5:715–726
14. Kralj S, Rojnik M, Jagodič M, Kos J, Makovec D (2012) Effect of surface charge on the cellular uptake of fluorescent magnetic nanoparticles. J Nanopart Res 14:1–14
15. Lu AH, Salabas EL, Schüth F (2007) Magnetic nanoparticles: synthesis, protection, functionalization, and application. Angew Chem Int Ed Engl 46(8):1222–1244
16. Johnson SH, Johnson CL, May SJ, Hirsch S, Cole MW, Spanier JE (2009) Co@ CoO@ Au core-multi-shell nanocrystals. J Mater Chem 20:439–443
17. Grass RN, Stark WJ (2006) Gas phase synthesis of fcc-cobalt nanoparticles. J Mater Chem 16:1825–1830
18. Shafi KVPM, Ulman A, Yan X, Yang N-L, Estournes C, White H et al (2001) Sonochemical synthesis of functionalized amorphous iron oxide nanoparticles. Langmuir 17(16):5093–5097
19. Sjøgren CE, Briley-Saebø K, Hanson M, Johansson C (1994) Magnetic characterization of iron oxides for magnetic resonance imaging. Magn Reson Med 31(3):268–272
20. Jiang W, Yang H-C, Yang S-Y, Horng H-E, Hung JC, Chen YC et al (2004) Preparation and properties of superparamagnetic nanoparticles with narrow size distribution and biocompatible. J Magn Magn Mater 283(2–3):210–214
21. Gupta AK, Wells S (2004) Surface-modified superparamagnetic nanoparticles for drug delivery: preparation, characterization, and cytotoxicity studies. IEEE Trans Nanobioscience 3(1):66–73
22. Wang X, Zhuang J, Peng Q, Li Y (2005) A general strategy for nanocrystal synthesis. Nature 437:121–124
23. Peng X, Wickham J, Alivisatos AP (1998) Kinetics of II–VI and III–V colloidal semiconductor nanocrystal growth: "Focusing" of size distributions. J Am Chem Soc 120(21):5343–5344

24. Samia ACS, Hyzer K, Schlueter JA, Qin C-J, Jiang JS, Bader SD et al (2005) Ligand effect on the growth and the digestion of Co nanocrystals. Am Chem Soc 127(12):4126–4127
25. Li Y, Afzaal M, O'Brien P (2006) The synthesis of amine-capped magnetic (Fe, Mn, Co, Ni) oxide nanocrystals and their surface modification for aqueous dispersibility. J Mater Chem 16:2175–2180
26. Farrell D, Majetich SA, Wilcoxon JP (2003) Preparation and characterization of monodisperse Fe nanoparticles. Phys Chem B 107(40):11022–11030
27. Sun S, Zeng H (2002) Size-controlled synthesis of magnetite nanoparticles. J Am Chem Soc 124(28):8204–8205
28. Li Z, Kawashita M, Araki N, Mitsumori M, Hiraoka M, Doi M (2011) Preparation of magnetic iron oxide nanoparticles for hyperthermia of cancer in a $FeCl_2$-$NaNO_3$-NaOH aqueous system. J Biomater Appl 25(7):643–661
29. Park J, Lee E, Hwang NM, Kang M, Kim SC, Hwang Y et al (2005) One-nanometer-scale size-controlled synthesis of monodisperse magnetic Iron oxide nanoparticles. Angew Chem Int Ed Engl 44(19):2932–2937
30. Li Z, Sun Q, Gao M (2004) Preparation of water-soluble magnetite nanocrystals from hydrated ferric salts in 2-pyrrolidone: mechanism leading to Fe_3O_4. Angew Chem Int Ed Engl 44(1):123–126
31. Hu FQ, Wei L, Zhou Z, Ran YL, Li Z, Gao MY (2006) Preparation of biocompatible magnetite nanocrystals for in vivo magnetic resonance detection of cancer. Adv Mater 18(19):2553–2556
32. Rosensweig RE (2002) Heating magnetic fluid with alternating magnetic field. J Magn Magn Mater 252:370–374
33. Dumestre F, Chaudret B, Amiens C, Renaud P, Fejes P (2004) Superlattices of iron nanocubes synthesized from Fe $[N(SiMe_3)_2]_2$. Science 303(5659):821–823
34. Song Q, Zhang ZJ (2004) Shape control and associated magnetic properties of spinel cobalt ferrite nanocrystals. J Am Chem Soc 126(19):6164–6168
35. Puntes VF, Krishnan KM, Alivisatos AP (2001) Colloidal nanocrystal shape and size control: the case of cobalt. Science 291(5511):2115–2117
36. Dumestre F, Chaudret B, Amiens C, Respaud M, Fejes P, Renaud P et al (2003) Unprecedented Crystalline Super-Lattices of Monodisperse Cobalt Nanorods. Angew Chem Int Ed Engl 42(42):5213–5216
37. Cordente N, Respaud M, Fo S, Casanove M-J, Amiens C, Chaudret B (2001) Synthesis and magnetic properties of nickel nanorods. Nano Lett 1(10):565–568
38. Sun S, Murray CB, Weller D, Folks L, Moser A (2000) Monodisperse FePt nanoparticles and ferromagnetic FePt nanocrystal superlattices. Science 287(5460):1989–1992
39. Tegus O, Brük E, Buschow KHJ, De Boer FR (2002) Transition-metal-based magnetic refrigerants for room-temperature applications. Nature 415:150–152
40. Perera SC, Tsoi G, Wenger LE, Brock SL (2003) Synthesis of MnP nanocrystals by treatment of metal carbonyl complexes with phosphines: a new, versatile route to nanoscale transition metal phosphides. J Am Chem Soc 125(46):13960–13961
41. Qian C, Kim F, Ma L, Tsui F, Yang P, Liu J (2004) Solution-phase synthesis of single-crystalline iron phosphide nanorods/nanowires. J Am Chem Soc 126(4):1195–1198
42. McCarthy JR, Weissleder R (2008) Multifunctional magnetic nanoparticles for targeted imaging and therapy. Adv Drug Deliv Rev 60(11):1241–1251
43. Ling D, Hyeon T (2013) Chemical design of biocompatible iron oxide nanoparticles for medical applications. Small 9(9–10):1450–1466
44. Nazli C, Ergenc TI, Yar Y, Acar HY, Kizilel S (2012) RGDS-functionalized polyethylene glycol hydrogel-coated magnetic iron oxide nanoparticles enhance specific intracellular uptake by HeLa cells. Int J Nanomedicine 7:1903–1920
45. Mahmoudi M, Sant S, Wang B, Laurent S, Sen T (2011) Superparamagnetic iron oxide nanoparticles (SPIONs): development, surface modification and applications in chemotherapy. Adv Drug Deliv Rev 63(1–2):24–46

46. Neuberger T, Schöpf B, Hofmann H, Hofmann M, Von Rechenberg B (2005) Superparamagnetic nanoparticles for biomedical applications: possibilities and limitations of a new drug delivery system. J Magn Magn Mater 293(1):483–496
47. Kataby G, Ulman A, Prozorov R, Gedanken A (1998) Coating of amorphous iron nanoparticles by long-chain alcohols. Langmuir 14(7):1512–1515
48. Anbarasu M, Anandan M, Chinnasamy E, Gopinath V, Balamurugan K (2015) Synthesis and characterization of polyethylene glycol (PEG) coated Fe_3O_4 nanoparticles by chemical co-precipitation method for biomedical applications. Spectrochim Acta A Mol Biomol Spectrosc 135:536–539
49. Masoudi A, Hosseini HRM, Shokrgozar MA, Ahmadi R, Oghabian MA (2012) The effect of poly (ethylene glycol) coating on colloidal stability of superparamagnetic iron oxide nanoparticles as potential MRI contrast agent. Int J Pharm 433(1–2):129–141
50. Demirer GS, Okur AC, Kizilel S (2015) Synthesis and design of biologically inspired biocompatible iron oxide nanoparticles for biomedical applications. J Mater Chem B 3:7831–7849
51. Rahman MM, Afrin S, Haque P (2014) Characterization of crystalline cellulose of jute reinforced poly (vinyl alcohol)(PVA) biocomposite film for potential biomedical applications. Progress Biomater 3:1–9
52. Zhang Y, Kohler N, Zhang M (2002) Surface modification of superparamagnetic magnetite nanoparticles and their intracellular uptake. Biomaterials 23(7):1553–1561
53. Shubayev VI, Pisanic TR, Jin S (2009) Magnetic nanoparticles for theragnostics. Adv Drug Deliv Rev 61(6):467–477
54. Shagholani H, Ghoreishi SM, Mousazadeh M (2015) Improvement of interaction between PVA and chitosan via magnetite nanoparticles for drug delivery application. Int J Biol Macromol 78:130–136
55. Zhu X-M, Wang YX, Leung KC, Lee S-F, Zhao F, Wang D-W et al (2012) Enhanced cellular uptake of aminosilane-coated superparamagnetic iron oxide nanoparticles in mammalian cell lines. Int J Nanomedicine 7:953–964
56. Gupta AK, Gupta M (2005) Synthesis and surface engineering of iron oxide nanoparticles for biomedical applications. Biomaterials 26(18):3995–4021
57. Du L, Chen J, Qi Y, Li D, Yuan C, Lin MC et al (2007) Preparation and biomedical application of a non-polymer coated superparamagnetic nanoparticle. Int J Nanomedicine 2(4):805–812. http://www.dovepress.com/articles.php?journal_id=5
58. Josephson L, Tung C-H, Moore A, Weissleder R (1999) High-efficiency intracellular magnetic labeling with novel superparamagnetic-Tat peptide conjugates. Bioconjug Chem 10(2):186–191
59. Jafari A, Salouti M, Shayesteh SF, Heidari Z, Rajabi AB, Boustani K et al (2015) Synthesis and characterization of Bombesin-superparamagnetic iron oxide nanoparticles as a targeted contrast agent for imaging of breast cancer using MRI. Nanotechnology 26(7):075101
60. Zeng L, Piao Z, Huang S, Jia W, Chen Z (2015) Label-free optical-resolution photoacoustic microscopy of superficial microvasculature using a compact visible laser diode excitation. Opt Express 23(24):31026–31033
61. Xu M, Wang LV (2006) Photoacoustic imaging in biomedicine. Rev Sci Instrum 77:041101
62. Zhang Y, Hong H, Cai W. Photoacoustic imaging. Cold Spring Harbor Laboratory Press. p. pdb. top065508.
63. Wang X, Pang Y, Ku G, Stoica G, Wang LV (2003) Three-dimensional laser-induced photoacoustic tomography of mouse brain with the skin and skull intact. Opt Lett 28(19):1739–1741
64. Oh J-T, Li M-L, Zhang HF, Maslov K, Stoica G, Wang LV (2006) Three-dimensional imaging of skin melanoma in vivo by dual-wavelength photoacoustic microscopy. J Biomed Opt 11(3):034032–034034
65. Shashkov EV, Everts M, Galanzha EI, Zharov VP (2008) Quantum dots as multimodal photoacoustic and photothermal contrast agents. Nano Lett 8(11):3953–3958
66. Luke GP, Yeager D, Emelianov SY (2012) Biomedical applications of photoacoustic imaging with exogenous contrast agents. Ann Biomed Eng 40(2):422–437

67. Jin Y, Jia C, Huang S-W, O'Donnell M, Gao X (2010) Multifunctional nanoparticles as coupled contrast agents. Nat Commun 1:41
68. Xu Z, Hou Y, Sun S (2007) Magnetic core/shell Fe_3O_4/Au and Fe_3O_4/Au/Ag nanoparticles with tunable plasmonic properties. J Am Chem Soc 129(28):8698–8699
69. Ji X, Shao R, Elliott AM, Stafford RJ, Esparza-Coss E, Bankson JA et al (2007) Bifunctional gold nanoshells with a superparamagnetic iron oxide-silica core suitable for both MR imaging and photothermal therapy. J Phys Chem C 111(17):6245–6251
70. Tartaj P, del Puerto MM, Veintemillas-Verdaguer S, González-Carreño T, Serna CJ (2003) The preparation of magnetic nanoparticles for applications in biomedicine. J Phys D Appl Phys 42(22):R182
71. Basuki JS, Esser L, Zetterlund PB, Whittaker MR, Boyer C, Davis TP (2013) Grafting of P (OEGA) onto magnetic nanoparticles using Cu (0) mediated polymerization: comparing grafting "from" and "to" approaches in the search for the optimal material design of nanoparticle MRI contrast agents. Macromolecules 46(15):6038–6047
72. Mandal S, Chatterjee N, Das S, Saha KD, Chaudhuri K (2014) Magnetic core–shell nanoprobe for sensitive killing of cancer cells via induction with a strong external magnetic field. RSC Adv 4:20077–20085
73. Basuki JS, Jacquemin A, Esser L, Li Y, Boyer C, Davis TP (2014) A block copolymer-stabilized co-precipitation approach to magnetic iron oxide nanoparticles for potential use as MRI contrast agents. Polym Chem 5:2611–2620
74. Bremerich J, Bilecen D, Reimer P (2007) MR angiography with blood pool contrast agents. Eur Radiol 17(12):3017–3024
75. Ito A, Shinkai M, Honda H, Kobayashi T (2005) Medical application of functionalized magnetic nanoparticles. J Biosci Bioeng 100(1):1–11
76. Mandal S, Chaudhuri K (2016) Engineered magnetic core shell nanoprobes: synthesis and applications to cancer imaging and therapeutics. World J Biol Chem 7(1):158–167
77. Sb B, Laurent S, Elst LV, Muller RN (2006) Specific E-selectin targeting with a superparamagnetic MRI contrast agent. Contrast Media Mol Imaging 1(1):15–22
78. Yu MK, Jeong YY, Park J, Park S, Kim JW, Min JJ et al (2008) Drug-loaded superparamagnetic iron oxide nanoparticles for combined cancer imaging and therapy in vivo. Angew Chem Int Ed Engl 47(29):5362–5365
79. Yang X, Hong H, Grailer JJ, Rowland IJ, Javadi A, Hurley SA et al (2011) cRGD-functionalized, DOX-conjugated, and 64 Cu-labeled superparamagnetic iron oxide nanoparticles for targeted anticancer drug delivery and PET/MR imaging. Biomaterials 32(17):4151–4160
80. Orive G, Hernandez RM, Rodríguez Gascón A, Domínguez-Gil A, Pedraz JL (2003) Drug delivery in biotechnology: present and future. Curr Opin Biotechnol 14(6):659–664
81. Colombo M, Carregal-Romero S, Casula MF, Gutierrez L, Morales MP, Boehm IB et al (2012) Biological applications of magnetic nanoparticles. Chem Soc Rev 41:4306–4334
82. Mashhadizadeh MH, Amoli-Diva M (2013) Atomic absorption spectrometric determination of Al^{3+} and Cr^{3+} after preconcentration and separation on 3-mercaptopropionic acid modified silica coated-Fe_3O_4 nanoparticles. J Anal At Spectrom 28:251–258
83. Kievit FM, Wang FY, Fang C, Mok H, Wang K, Silber JR et al (2011) Doxorubicin loaded iron oxide nanoparticles overcome multidrug resistance in cancer in vitro. J Control Release 152(1):76–83
84. Chomoucka J, Drbohlavova J, Huska D, Adam V, Kizek R, Hubalek J (2010) Magnetic nanoparticles and targeted drug delivering. Pharmacol Res 62(2):144–149
85. N'Guyen TTT, Duong HTT, Basuki J, Vr M, Pascual S, Cm G et al (2013) Functional iron oxide magnetic nanoparticles with hyperthermia-induced drug release ability by using a combination of orthogonal click reactions. Angew Chem Int Ed Engl 52(52):14152–14156
86. McBain SC, Yiu HHP, Dobson J (2008) Magnetic nanoparticles for gene and drug delivery. Int J Nanomedicine 3(2):169–180

87. Wilson MW, Kerlan RK Jr, Fidelman NA, Venook AP, LaBerge JM, Koda J et al (2004) Hepatocellular carcinoma: regional therapy with a magnetic targeted carrier bound to doxorubicin in a dual MR imaging/conventional angiography suite–initial experience with four patients. Radiology 230(1):287–293
88. Basuki JS, Duong HTT, Macmillan A, Erlich RB, Esser L, Akerfeldt MC et al (2013) Using fluorescence lifetime imaging microscopy to monitor theranostic nanoparticle uptake and intracellular doxorubicin release. ACS Nano 7(11):10175–10189
89. Laurent S, Dutz S, Häfeli UO, Mahmoudi M (2011) Magnetic fluid hyperthermia: focus on superparamagnetic iron oxide nanoparticles. Adv Colloid Interface Sci 166(1–2):8–23
90. Shen J-M, Guan X-M, Liu X-Y, Lan J-F, Cheng T, Zhang H-X (2012) Luminescent/magnetic hybrid nanoparticles with folate-conjugated peptide composites for tumor-targeted drug delivery. Bioconjug Chem 23(5):1010–1021
91. Kebede A, Singh AK, Rai PK, Giri NK, Rai AK, Watal G et al (2013) Controlled synthesis, characterization, and application of iron oxide nanoparticles for oral delivery of insulin. Lasers Med Sci 28(2):579–587
92. Shen J-M, Xu L, Lu Y, Cao H-M, Xu Z-G, Chen T et al (2012) Chitosan-based luminescent/magnetic hybrid nanogels for insulin delivery, cell imaging, and antidiabetic research of dietary supplements. Int J Pharm 427(2):400–409
93. Yu MK, Kim D, Lee IH, So JS, Jeong YY (2011) Jon S. Image-guided prostate cancer therapy using aptamer-functionalized thermally cross-linked superparamagnetic iron oxide nanoparticles. Small 7(15):2241–2249
94. Chen F-H, Zhang L-M, Chen Q-T, Zhang Y, Zhang Z-J (2010) Synthesis of a novel magnetic drug delivery system composed of doxorubicin-conjugated Fe_3O_4 nanoparticle cores and a PEG-functionalized porous silica shell. Chem Commun (Camb) 46(45):8633–8635
95. Kruse AM, Meenach SA, Anderson KW, Hilt JZ (2014) Synthesis and characterization of CREKA-conjugated iron oxide nanoparticles for hyperthermia applications. Acta Biomater 10(6):2622–2629
96. Zhao M, Kircher MF, Josephson L, Weissleder R (2002) Differential conjugation of tat peptide to superparamagnetic nanoparticles and its effect on cellular uptake. Bioconjug Chem 13(4):840–844
97. Strable E, Bulte JWM, Moskowitz B, Vivekanandan K, Allen M, Douglas T (2001) Synthesis and characterization of soluble iron oxide-dendrimer composites. Chem Mater 13(6):2201–2209
98. Bulte JWM, Kraitchman DL (2004) Iron oxide MR contrast agents for molecular and cellular imaging. NMR Biomed 17(7):484–499
99. Lu C-W, Hung Y, Hsiao J-K, Yao M, Chung T-H, Lin Y-S et al (2007) Bifunctional magnetic silica nanoparticles for highly efficient human stem cell labeling. Nano Lett 7(1):149–154
100. Arbab AS, Yocum GT, Kalish H, Jordan EK, Anderson SA, Khakoo AY et al (2004) Efficient magnetic cell labeling with protamine sulfate complexed to ferumoxides for cellular MRI. Blood 104(4):1217–1223
101. Yeh TC, Zhang W, Ildstad ST, Ho C (1995) In vivo dynamic MRI tracking of rat T-cells labeled with superparamagnetic iron-oxide particles. Magn Reson Med 33(2):200–208
102. Dodd CH, Hsu H-C, Chu W-J, Yang P, Zhang H-G, Mountz JD et al (2001) Normal T-cell response and in vivo magnetic resonance imaging of T cells loaded with HIV transactivator-peptide-derived superparamagnetic nanoparticles. J Immunol Methods 256(1–2):89–105
103. Cherukuri P, Glazer ES, Curley SA (2010) Targeted hyperthermia using metal nanoparticles. Adv Drug Deliv Rev 62(3):339–345
104. Chatterjee DK, Diagaradjane P, Krishnan S (2011) Nanoparticle-mediated hyperthermia in cancer therapy. Ther Deliv 2(8):1001–1014
105. Silva AC, Oliveira TR, Mamani JB, Malheiros SMF, Malavolta L, Pavon LF et al (2011) Application of hyperthermia induced by superparamagnetic iron oxide nanoparticles in glioma treatment. Int J Nanomedicine 6:591–603
106. Johannsen M, Thiesen B, Wust P, Jordan A (2010) Magnetic nanoparticle hyperthermia for prostate cancer. Int J Hyperthermia 26(8):790–795

107. Johannsen M, Gneveckow U, Eckelt L, Feussner A, Waldöfner N, Scholz R et al (2005) Clinical hyperthermia of prostate cancer using magnetic nanoparticles: presentation of a new interstitial technique. Int J Hyperthermia 21(7):637–647
108. Gordon AC, Lewandowski RJ, Salem R, Day DE, Omary RA, Larson AC (2014) Localized hyperthermia with iron oxide-doped yttrium microparticles: steps toward image-guided thermoradiotherapy in liver cancer. J Vasc Interv Radiol 25(3):397–404
109. Hayashi K, Ono K, Suzuki H, Sawada M, Moriya M, Sakamoto W et al (2010) High-frequency, magnetic-field-responsive drug release from magnetic nanoparticle/organic hybrid based on hyperthermic effect. ACS Appl Mater Interfaces 2(7):1903–1911
110. Dobbrow C, Schmidt AM (2012) Improvement of the oxidation stability of cobalt nanoparticles. Beilstein J Nanotechnol 3:75–81
111. Hergt R, Dutz S (2007) Magnetic particle hyperthermia—biophysical limitations of a visionary tumour therapy. J Magn Magn Mater 311(1):187–192
112. Walther W, Siegel R, Kobelt D, Knösel T, Dietel M, Bembenek A et al (2008) Novel jet-injection technology for nonviral intratumoral gene transfer in patients with melanoma and breast cancer. Clin Cancer Res 14(22):7545–7553
113. Cederfjäll E, Sahin G, Kirik D (2012) Key factors determining the efficacy of gene therapy for continuous DOPA delivery in the Parkinsonian brain. Neurobiol Dis 48(2):222–227
114. Huschka R, Barhoumi A, Liu Q, Roth JA, Ji L, Halas NJ (2012) Gene silencing by gold nanoshell-mediated delivery and laser-triggered release of antisense oligonucleotide and siRNA. ACS Nano 6(9):7681–7691
115. Dobson J (2006) Gene therapy progress and prospects: magnetic nanoparticle-based gene delivery. Gene Ther 13(4):283–287
116. Boyer C, Priyanto P, Davis TP, Pissuwan D, Bulmus V, Kavallaris M et al (2010) Anti-fouling magnetic nanoparticles for siRNA delivery. J Mater Chem 20:255–265
117. Yu-Feng T, Shu-Jun H, Shi-Shen Y, Liang-Mo M (2013) Oxide magnetic semiconductors: materials, properties, and devices. Chinese Physics B 22(8):088505
118. Mah C, Fraites TJ Jr, Zolotukhin I, Song S, Flotte TR, Dobson J et al (2002) Improved method of recombinant AAV2 delivery for systemic targeted gene therapy. Mol Ther 6(1):106–112
119. Safarik I, Safarikova M (2004) Magnetic techniques for the isolation and purification of proteins and peptides. Biomagn Res Technol 2:1
120. Widjojoatmodjo MN, Fluit AC, Torensma R, Verhoef J (1993) Comparison of immunomagnetic beads coated with protein A, protein G, or goat anti-mouse immunoglobulins Applications in enzyme immunoassays and immunomagnetic separations. J Immunol Methods 165(1):11–19
121. Fan J, Lu J, Xu R, Jiang R, Gao Y (2003) Use of water-dispersible Fe_2O_3 nanoparticles with narrow size distributions in isolating avidin. J Colloid Interface Sci 266(1):215–218
122. Nagatani N, Shinkai M, Honda H, Kobayashi T (1998) Development of a new transformation method using magnetite cationic liposomes and magnetic selection of transformed cells. Biotech Techn 12(7):525–528
123. Lobel B, Eyal O, Kariv N, Katzir A (2000) Temperature controlled CO_2 laser welding of soft tissues: urinary bladder welding in different animal models (rats, rabbits, and cats). Lasers Surg Med 26(1):4–12
124. Dew DK, Supik L, Darrow CR, Price GF (1993) Tissue repair using lasers: a review. Orthopedics 16(5):581–587
125. Domenech M, Marrero-Berrios I, Torres-Lugo M, Rinaldi C (2013) Lysosomal membrane permeabilization by targeted magnetic nanoparticles in alternating magnetic fields. ACS Nano 7(6):5091–5101
126. Choi J, Shin J, Lee J, Cha M (2012) Magnetic response of mitochondria-targeted cancer cells with bacterial magnetic nanoparticles. Chem Commun 48:7474–7476